A Mushy Region in Concrete Corrosion

C. V. Nikolopoulos

Department of Mathematics, University of the Aegean,
Karlovasi, 83200, Samos, Greece.

Abstract

In this work a mathematical model already known for the corrosion of sewer pipes is further considered, enriched and an approximate analytical solution is given based on a quasi steady approximation. Furthermore an extension of this model is constructed allowing the formation of a mushy region, i.e. a region in which the material is only partly corroded throughout the process. This more general model is derived via an averaging process by microscopic considerations and has the form of a macroscopic phase field model. The derived model in its various forms is solved numerically with a finite element method and the results, predicting corrosion within a reasonable range, are presented.

Key words: Sulfide Corrosion, Concrete Corrosion, Free Boundary Problems, Perturbation methods.

1 Introduction

A model regarding transport of sewage in sewer pipes which leads to the release of hydrogen sulfide (H_2S) and reacts to form a corrosive compound (H_2SO_4) in sewers is considered in [4]. More specifically, in [4], biological generation of SO_4^- from H_2S and transport of H_2S and SO_4^- from the interior of the pipe to the corrosion front separating corroded and uncorroded parts of the pipe walls, is modelled by a system of three weakly coupled reaction - diffusion equations. The model is presented initially in [4] and it is also studied in [5]. Existence and uniquiness of the system is studied in [12]. Some experimental results regarding corrosion of sewer pipes are also presented in [3].

The basic reaction that it is considered, expressing the actual fact that H_2SO_4 reacts with calsite $CaCO_3$ forming gypsum $CaSO_4 \cdot 2H_2O$ and causing the

Email address: cnikolo@aegean.gr (C. V. Nikolopoulos).

corrosion of the concrete, is the following:

$$2H_2O + H^+ + SO_4^{2-} + CaCO_3 \xrightarrow{K_c} CaSO_4 \cdot 2H_2O + HCO_3^-.$$

As it is also addressed in [4] a model considering the formation of a mushy region should be useful, giving a more realistic approach to the phenomenon. A mushy region in this case would mean to have both uncorroded and corroded parts of the material coexisting during the process in an element volume of it and not having a distinct macroscopic interface separating the corroded and uncorroded parts of the material.

Note that the aforementioned chemical reaction is the same when we consider for example corrosion due to H_2S of marble of antiquities or of similar physical systems. More specifically a series of studies for the chemical aggregation of limestones (corrosion of antiquities), which in its basis it is a similar phenomenon, has been presented in a series of papers as in [1], [2], [8], [9], [10]. With minor modifications the models derived in this work can also be adopted in the case that we study corrosion of marbles from atmospheric pollution or other physical systems as well (see [9] etc.). Note that in these models it is assumed a linear dependence of the porosity from the calcite concentration while in the present work the dependence of the porosity from the calcite concentration comes from a differential equation which is derived from specific considerations for the microstructure of the system.

In the present work as an example of a physical system, illustrating how a model which accounts for the formation of a mushy region can be derived, we will use as a base the model derived in [4]. Initially, in Section 2, we will present it and give a brief explanation of how the equations of the model are derived. Then we apply a nondimensionalization to simplify the set of equations and in order to have an overview of the behaviour of the solution of the equation, additional to the results presented in [4], we apply the quasi steady approximation (omitted in [4]) to give an analytical approximation of the solution for some suitable range of the parameters of the model.

Having already some overview of this initial model we then apply the method of multiple scales to construct a phase field model derived from microstructure considerations in Section 3. This is motivated by a method initially presented in [13] and [14] which is adopted and modified appropriately to analyze the problem in our case. In order to do that we will consider inside the concrete and in the microstructure scale, cracks being parallel between them (in one and two - dimensional consideration) and equally spaced. The derived phase field models are presented in Section 3. In Section 4 the basic equation derived is solved numerically via a finite element method. The same method is applied to solve numerically the corresponding system of equations in the case that we

study the corrosion of the sewer pipes. This is also done for the case that this system is simplified with the use of the quasi steady approximation. Finally the conclusions of this work are presented in Section 5.

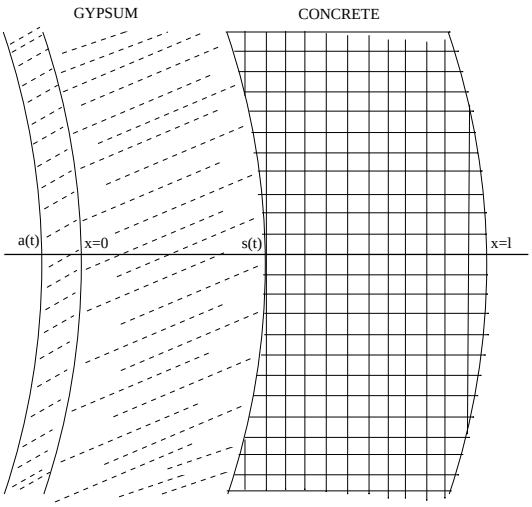

Fig. 1. *Schematic representation of a sewer pipe corrosion*

2 Presentation of the model and the Quasi Steady Approximation

The governing chemical reactions leading to the corrosion of sewer pipes (see [4]) are the following:

$$
\begin{aligned}
10\mathrm{H}^+ + \mathrm{SO}_4^{2-} + \text{org. matter} &\longrightarrow \mathrm{H_2S} + 4\mathrm{H_2O} + \text{oxidized org. matter} \\
\mathrm{H_2S} + 2\mathrm{O_2} &\xrightarrow{K_B} 2\mathrm{H}^+ + \mathrm{SO}_4^{2-} \\
2\mathrm{H_2O} + \mathrm{H}^+ + \mathrm{SO}_4^{2-} + \mathrm{CaCO_3} &\xrightarrow{K_c} \mathrm{CaSO_4 \cdot 2H_2O} + \mathrm{HCO_3^-}\,.
\end{aligned}
$$

We denote by u, v and w the concentrations of H_2S in the gaseous phase, of H_2S in the liquid phase and of SO_4^{2-} respectively, i.e. $u := [\mathrm{H_2S}]_{\mathrm{g}}$, $v := [\mathrm{H_2S}]_{\mathrm{aq}}$ and $w := [\mathrm{SO}_4^{2-}]$, where $[\,\cdot\,]$ denotes the concentration, the subscript g the gaseous phase, while the subscript aq stands for water. The constants K_B and K_c are the bio-conversion rate constant and the constant of reaction (dissolution rate constant) respectively (see [4]). The gypsum - concrete interface is represented by $x = s(t)$, for x measuring distance from the inner side of the wall and it is a nondecreasing function of time representing the progress of the corrosion inside the concrete. Also we may consider a second moving

boundary determining the motion of the outer surface of the material which is being corroded, denoted by $a(t)$, with $a(0)$=0 and which expresses the expansion of volume of the concrete-gypsum system, coming from the fact that the formed gypsum has lower density than the concrete. Now if we consider a one - dimensional movement of the corrosion front and if $\Omega(t) = (a(t), s(t))$, the interval which determines the corroded part of the material i.e. the gypsum part, then the equations for u, v and w are the following (see [4])

$$
\begin{aligned}
u_t &= D_a u_{xx} + P_u, \\
v_t &= D_w v_{xx} + P_{v_1} + P_{v_2}, \\
w_t &= D_H w_{xx} + P_{w_1} + P_{w_2}.
\end{aligned}
$$

with

$$
\begin{aligned}
u(a(t), t) &= \lambda_1, \qquad & u_x(s(t), t) &= 0, \\
v(a(t), t) &= \lambda_2, \qquad & v_x(s(t), t) &= 0, \\
w(a(t), t) &= \lambda_3, \qquad & D_H w_x(s(t), t) &+ K_c \left(w(s(t), t)\right)^m = 0.
\end{aligned}
$$

where D_a, D_w, D_H are the diffusion coefficients and $P_u, P_{v_1}, P_{v_2}, P_{w_1}, P_{w_2}$ are various source terms which will be specified in the following. There is also need for the moving boundaries $a(t)$, and $s(t)$ to be specified by some additional equations which also will be given in the following. In addition we assume Dirichlet boundary conditions at the one end, $a(t)$ and Neumann conditions at the moving boundary $s(t)$, except for w where we have that the flow of w supplies with material the chemical reaction which transforms concrete into gypsum so that a condition of Robin type is posed instead. Actually the Robin boundary condition follow from the assumption that the calcite to gypsum reaction will go to completion whenever there is a non-negligible consentration of sulphate ions (fast reaction) and therefore we can consider that the reaction is happening at the surface separating calcite from gypsum.

As an initial approximation we may take $a(t) = 0$, for $t \geq 0$ accounting for the fact that the volume expansion of the material, due to the corrosion process, is negligible. Note also that regarding the diffusivities we have $D_a = T_a V_a D_{ha}$, $D_w = T_a V_w D_{hw}$, $D_H = T_a V_w D_{saw}$ where V_a, V_w are the porosities of the air and the water filled regions respectively, D_a, D_w, D_{saw} are the diffusion rates for u, v and w respectively and T_a is the tortuosity. We then focus our attention on the source terms. The term P_u expresses the exchange of H_2S between the air and the water phase, i.e.

$$P_u = -\frac{K_T A_S}{V_a}(K_{HS}u - v),$$

where
K_T is the mass transfer coefficient,
A_S is the surface area,
V_a is the porosity, fraction of volume of air filled pores,
K_{HS} is the Henry's law constant.

The term P_{v_1}, similarly, expresses the exchange of H_2S between the water and the air phase (inverse process of the one expressed by P_u), i.e.

$$P_{v_1} = \frac{K_T A_S}{V_w}(K_{HS}u - v),$$

where
V_w is the porosity, fraction of volume of water filled pores.
In addition the term P_{v_2} expresses the bioconversion of H_2S, that is,

$$P_{v_2} = -K_B v.$$

Also in the equation for w we have that $P_{w_1} = -P_{v_2}$, i.e. H_2S is giving SO_4^{2-} due to bioconversion and the term P_{w_2} expresses absorption of H_2S due to reaction with residues of $CaCO_3$ in water filled pores. In such a case we have

$$P_{w_2} = -K_c w^m C_c^n,$$

for C_c being the concentration of calcite, K_c the reaction constant and m, n the orders of the reactions.

If we assume that the reaction is complete at the boundary we have $P_{w_2} = 0$, i.e. no $CaCO_3$ is left after the reaction.

In the following we will therefore use the assumption that $P_{w_2} = 0$ where $w > 0$.

Therefore the resulting set of equations has the form

$$u_t = D_a u_{xx} - \frac{K_T A_S}{V_a}(K_{HS}u - v), \tag{2.1a}$$

$$v_t = D_w v_{xx} + \frac{K_T A_S}{V_w}(K_{HS} u - v) - K_B v, \tag{2.1b}$$

$$w_t = D_H w_{xx} + K_B v. \tag{2.1c}$$

The boundary conditions at $x = 0$, at $x = s(t)$ and the Stefan condition have the form

$$u(0,t) = \lambda_1, \quad v(0,t) = \lambda_2, \quad w(0,t) = \lambda_3, \tag{2.2a}$$

$$u_x(s(t),t) = 0, \;\; v_x(s(t),t) = 0, \;\; K_c\left(w(s(t),t)\right)^m + D_H w_x(s(t),t) = 0, \tag{2.2b}$$

$$\dot{s}(t) = \frac{K_c}{C_c} w^m, \tag{2.2c}$$

where K_c is the constant of reaction and m the reaction rate. Furthermore equation (2.2c) can be derived (see also [4]) by considering that $C_c \dot{s}(t)$ stands for the amount of calcium carbonate consumed per unit time which equals the reaction rate and thus $C_c \dot{s}(t) = K_c w^m$ or $\dot{s} = -P_{w_2}$ for $n = -1$. Also $\lambda_1, \lambda_2, \lambda_3$ are the given concentrations at $x = 0$.

These equations can be modified by dropping some of the assumptions we have adopted. More specifically in the case that we drop the assumptions regarding the outer free boundary $a(t)$ and the one regarding the source term P_{w_2} by taking $a(t) \neq 0$ and $P_{w_2} \neq 0$, the system takes the form of equations (2.1a), (2.1a) with the equation of w having the form

$$w_t = D_H w_{xx} + K_B v - K_c w^m C_c^n, \tag{2.3}$$

and with the addition also of an equation for the calcite variation. Possible convective terms resulting from the expansion of the material, i.e. from allowing $a(t) < 0$ can also be included in the equations for the concentrations. Although in this work when $a(t) \neq 0$ such terms will be considered negligible and not be taken into account (see also [4]).

In addition to the fact that we may take $a(t) \neq 0$ and $P_{w_2} \neq 0$ it is worth noting that also we can impose Robin boundary conditions at the left boundary , i.e.

$$u_x(a(t),t) = E_{up}(u - \lambda_1(t)), \tag{2.4a}$$

$$v_x(a(t),t) = E_{vl}(u - \lambda_2(t)), \tag{2.4b}$$

$$w_x(a(t),t) = E_{wl}(w - \lambda_3(t)), \tag{2.4c}$$

where E_{up}, E_{rl}, E_{wl}, are the mass transfer coefficients. In the rest of this work we will not consider these conditions in equation (2.4) and (2.3) and we will always assume Dirichlet conditions at the left boundary and that the reaction at the moving boundary is complete giving $P_{w_2} = 0$. Although the relevant analysis can be easily modified to include equation (2.4) instead of (2.2a) or the source term in equation (2.3).

Regarding now the $a(t) \neq 0$ case, at $x = s(t)$ we have similarly as before the boundary conditions to be given by the equations (2.2b), (2.2c) and the propagation of $a(t)$ to be given by the relation

$$\dot{a}(t) = \left(1 - \frac{\rho_c}{\rho_g}\right) \frac{k_c}{C_c} w(s(t), t)^m, \tag{2.5}$$

for ρ_c and ρ_g being the densities of the calcite and the gypsum respectively. This comes by a direct application of a conversation law (see [4]). In case that we take $\rho_c \neq \rho_g$, i.e. the calcium and the gypsum density to differ, we have $\rho_c \dot{s}(t) = \rho_g\Big(\dot{s}(t) - \dot{a}(t)\Big)$ and equation (2.5) is implied. Moreover as initial conditions for both cases (for $a = 0$ or $a \neq 0$) in order to complete the system of equations, we may take

$$u(x, 0) = 0, \quad v(x, 0) = 0, \quad w(x, 0) = 0. \tag{2.6}$$

Finally in the following and in the rest of this work, for simplicity reasons, we will assume as in [4] that $m = 1$.

Nondimensionalization We focus our attention to the system of equations (2.1), (2.2), (2.6) and we scale the problem by the use of appropriate constants. We scale x with l, $y = \frac{x}{l}$ where l is a typical length of the observed corrosion in a period of years. Also we scale u, v, w with λ_1, λ_2, λ_3 respectively and we have

$$U = \frac{u_1}{\lambda_1}, \quad V = \frac{v}{\lambda_2}, \quad W = \frac{w}{\lambda_3}, \quad S = \frac{s}{l}.$$

In addition we set $\tau = \frac{t}{t_0}$ for τ being the dimensional variable and for t_0 a typical time which will be chosen in such a way so that the terms in the equation of the moving boundary are balanced.

Therefore the equation for u becomes

$$\left(\frac{l^2}{D_a t_0}\right) \frac{\partial U}{\partial \tau} = \frac{\partial^2 U}{\partial y^2} - \left(\frac{K_T A_s \lambda_2}{V_a \lambda_1} \frac{l^2}{D_a}\right) \left(\frac{K_{HS} \lambda_1}{\lambda_2} U - V\right),$$

or

$$\epsilon_1 \frac{\partial U}{\partial \tau} = \frac{\partial^2 U}{\partial y^2} - \mu_1 \left(\beta_1 U - V\right), \quad 0 < y < S(\tau),$$

for $\epsilon_1 = \frac{l^2}{D_a t_0}$, $\mu_1 = \frac{K_T A_s \lambda_2 l^2}{V_a \lambda_1 D_a}$ and $\beta_1 = \frac{K_{HS} \lambda_1}{\lambda_2}$. Note that $\beta_1 = 1$ due to the fact that $K_{HS} \lambda_1 = \lambda_2$ for numbers given in [4].

In a similar way we deduce that

$$\epsilon_2 \frac{\partial V}{\partial \tau} = \frac{\partial^2 V}{\partial y^2} + \mu_2 (U - V) - \beta_2 V, \quad 0 < y < S(\tau),$$

for $\epsilon_2 = \frac{l^2}{D_w t_0}$, $\mu_2 = \frac{K_T A_s l^2}{V_w D_w}$ and $\beta_2 = \frac{k_B l^2}{D_w}$, and that

$$\epsilon_3 \frac{\partial W}{\partial \tau} = \frac{\partial^2 W}{\partial y^2} + \beta_3 V, \quad 0 < y < S(\tau),$$

for $\epsilon_3 = \frac{l^2}{D_H t_0}$, and $\beta_3 = \frac{k_B \lambda_2 l^2}{D_H \lambda_3}$.

Regarding the boundary conditions at $x = 0$ we have

$$U(0,t) = V(0,t) = W(0,t) = 1, \quad y \in (0, S(0)).$$

The boundary conditions at $y = S(\tau)$ now have the form

$$U_y(S(\tau),\tau) = 0, \quad V_y(S(\tau),\tau) = 0, \quad \gamma W_y(S(\tau),\tau) + W(S(\tau),\tau) = 0,$$

for $\gamma = \frac{D_H}{l K_c}$.

Finally the equation for $S(\tau)$ becomes

$$\dot{S}(\tau) = W(S(\tau),\tau),$$

for the appropriate choice of t_0, given by $t_0 = \frac{C_c l}{K_c \lambda_3}$.

Summarizing we have the system

$$\epsilon_1 \frac{\partial U}{\partial \tau} = \frac{\partial^2 U}{\partial y^2} - \mu_1 (U - V), \tag{2.7a}$$

$$\epsilon_2 \frac{\partial V}{\partial \tau} = \frac{\partial^2 V}{\partial y^2} + \mu_2 (U - V) - \beta_2 V, \tag{2.7b}$$

$$\epsilon_3 \frac{\partial W}{\partial \tau} = \frac{\partial^2 W}{\partial y^2} + \beta_3 V \tag{2.7c}$$

for $0 < y < S(\tau)$, with boundary conditions,

$$U(0,\tau) = 1, \qquad U_y(S(\tau),\tau) = 0, \tag{2.8a}$$

$$V(0,\tau) = 1, \qquad V_y(S(\tau),\tau) = 0, \tag{2.8b}$$

$$W(0,\tau) = 1, \qquad \gamma W_y(S(\tau),\tau) + W(S(\tau),\tau) = 0, \tag{2.8c}$$

the condition for the free boundary,

$$\dot{S}(\tau) = W(S(\tau),\tau), \quad S(0) = S_a, \tag{2.9}$$

for $\tau > 0$, some $S_a > 0$ and the initial conditions

$$U(y,0) = 0, \quad V(y,0) = 0, \quad W(y,0) = 0, \quad 0 < y < S(0). \tag{2.10}$$

Taking numbers by [4] we have for example that for $K_c = 0.0084$, $l = 2\,cm$ and the $D_i's, K_T, A_s, V_i's, K_B$ etc. taken as in [4] that $\epsilon_1 \simeq O(10^{-7})$, $\epsilon_2, \epsilon_3 \simeq O(10^{-3})$, while $\mu_1 \simeq 7.57\times10^5$, $\mu_2 \simeq 3.03\times10^9$ and $\beta_2 \simeq 2.52\times10^3$, $\beta_3 \simeq 0.025$, $\gamma \simeq 6.78$.

These sizes justify the use of the quasi-steady approximation for the problem. Note that this approximation would be useful in general for values of the parameters giving the $\epsilon's$ small and negligible in the set of equations (2.7). In other words it seems that for this physical system, for a time scale of years where the evolution of corrosion is observable, we have very fast diffusion together with very fast exchange of H_2S between the air and water filled pores. Indeed for $\epsilon_1, \epsilon_2, \epsilon_3 \ll 1$, $\mu_1, \mu_2 \gg 1$, $\beta_2 \gg 1$, we rewrite the equations in the following form

$$\begin{aligned}
\frac{\epsilon_1}{\mu_1}\frac{\partial U}{\partial \tau} &= \frac{1}{\mu_1}\frac{\partial^2 U}{\partial y^2} - (U - V)\,, \\
\frac{\epsilon_2}{\mu_2}\frac{\partial V}{\partial \tau} &= \frac{1}{\mu_2}\frac{\partial^2 V}{\partial y^2} + (U - V) - \frac{\beta_2}{\mu_2}V, \\
\epsilon_3\frac{\partial W}{\partial \tau} &= \frac{\partial^2 W}{\partial y^2} + \beta_3 V,
\end{aligned}$$

with the initial and boundary conditions given by equations (2.8), (2.9) and (2.10). We notice that $\frac{\beta_2}{\mu_2} = O(\frac{1}{\mu_1})$ so we can set for some $\nu_2 \simeq O(1)$ that $\frac{\beta_2}{\mu_2} = \nu_2\frac{1}{\mu_1}$.

We also set $\epsilon = \frac{1}{\sqrt{\mu_2}}$ and $\nu_1\epsilon = \frac{1}{\mu_1}$ for $\nu_1 = O(1)$. Thus we obtain

$$\epsilon_1\epsilon\nu_1\frac{\partial U}{\partial\tau}=\epsilon\nu_1\frac{\partial^2 U}{\partial y^2}-(U-V)\,,$$
$$\epsilon_2\epsilon^2\frac{\partial V}{\partial\tau}=\epsilon^2\frac{\partial^2 V}{\partial y^2}+(U-V)-\nu_2\nu_1\epsilon V,$$
$$\epsilon_3\frac{\partial W}{\partial\tau}=\frac{\partial^2 W}{\partial y^2}+\beta_3 V.$$

Note that, motivated by the numbers given in [4], we may take $\epsilon_1 \simeq O(\epsilon^2)$ and ϵ_2, $\epsilon_3 \simeq O(\epsilon)$. Therefore we may take an expansion of the form

$$U\sim U_0+\epsilon U_1+\epsilon^2 U_2+\ldots,$$
$$V\sim V_0+\epsilon V_1+\epsilon^2 V_2+\ldots,$$
$$W\sim W_0+\epsilon W_1+\epsilon^2 W_2+\ldots,$$
$$S\sim S_0+\epsilon S_1+\epsilon^2 S_2+\ldots,$$

and substituting these expressions for U and V to the relevant equations we get

$$\epsilon_1\epsilon\nu_1\left(U_{0\tau}+\epsilon U_{1\tau}+\ldots\right)=\nu_1\epsilon\left(U_{0yy}+\epsilon U_{1yy}+\ldots\right)-(U_0-V_0)$$
$$-\epsilon\left(U_1-V_1\right)-\ldots, \qquad (2.11)$$

$$\epsilon_2\epsilon^2\left(V_{0\tau}+\epsilon V_{1\tau}+\ldots\right)=\epsilon^2\left(V_{0yy}+\epsilon V_{1yy}+\ldots\right)+(U_0-V_0)+\epsilon\left(U_1-V_1\right)$$
$$-\nu_1\nu_2\epsilon V_0-\nu_1\nu_2\epsilon^2 V_1-\ldots, \qquad (2.12)$$

$$\epsilon_3\left(W_{0\tau}+\epsilon W_{1\tau}+\ldots\right)=\left(W_{0yy}+\epsilon W_{1yy}+\ldots\right)+\beta_3 V_0+\beta_3\epsilon V_1+\ldots\ . \qquad (2.13)$$

By equations (2.11) and (2.12) we obtain to $O(1)$ terms that

$$U_0-V_0=0.$$

Also by the fact that $\epsilon_3=O(\epsilon)\ll 1$ and by equation (2.13) we obtain to $O(1)$ terms

$$W_{0yy} + \beta_3 V_0 = 0. \tag{2.14}$$

Looking at the $O(\epsilon)$ terms we get by equations (2.11) and (2.12) that

$$\begin{aligned} &\nu_1 U_{0yy} - (U_1 - V_1) = 0, \\ &(U_1 - V_1) - \nu_1 \nu_2 V_0 = 0. \end{aligned}$$

Thus we get $U_1 - V_1 = \nu_1 \nu_2 V_0$ and as a consequence that

$$U_{0yy} - \nu_2 V_0 = 0,$$

or that

$$U_{0yy} - \nu_2 U_0 = 0, \quad \text{with} \quad U(0,\tau) = 1, \quad U_y(S_0(\tau),\tau) = 0.$$

This implies that the solution for U_0 is

$$U_0(y,\tau) = U_0(y;\, S_0(\tau)) = \frac{\cosh\left(\sqrt{\nu_2}(y - S_0(\tau))\right)}{\cosh\left(\sqrt{\nu_2} S_0(\tau)\right)},$$

and

$$U_0(y,\tau) = V_0(y,\tau).$$

Now regarding the dominant term in the expansion for W we have

$$W_{0yy} - \beta_3 V_0 = 0,$$

with boundary conditions, to leading order terms,

$$W_0(0,\tau) = 1, \quad \gamma W_{0y}(S_0(\tau),\tau) + W_0(S_0(\tau),\tau) = 0.$$

In addition we also have

$$\dot{S}_0(\tau) = W_0(S_0(\tau), \tau).$$

Then the solution for W_0 is

$$\begin{aligned} W_0(y,\tau) = & \frac{\nu_2+\beta_3}{\nu_2(S_0(\tau)+\gamma)}\left[S_0(\tau)-y+\gamma\right] \\ & + \frac{\beta_3}{\nu_2(S_0(\tau)+\gamma)}\left[y-(S_0(\tau)+\gamma)\mathrm{sech}\left(\sqrt{\nu_2}(S_0(\tau)-y)\right)\right]\mathrm{sech}\left(\sqrt{\nu_2}S_0(\tau)\right). \end{aligned}$$

More specifically for $y = S(\tau) \simeq S_0(\tau)$ we get

$$W_0(S_0(\tau),\tau) = \frac{\gamma(\nu_2+\beta_3) - \beta_3\gamma\,\mathrm{sech}\left(\sqrt{\nu_2}S_0(\tau)\right)}{\nu_2(S_0(\tau)+\gamma)},$$

and the resulting equation for S to leading order terms has the form of an ordinary differential equation. Indeed we obtain that

$$\frac{dS(\tau)}{d\tau} = \frac{\gamma(\nu_2+\beta_3) - \beta_3\gamma\,\mathrm{sech}\left(\sqrt{\nu_2}S(\tau)\right)}{\nu_2(S(\tau)+\gamma)}, \tag{2.15}$$

with $S(0) = S_a$. This equation can be solved easily numerically e.g. via a Runge-Kutta scheme, and in Figure (2) we can see the motion of the moving boundary. The result is in very good agreement with the relevant result in [4] which is produced by the numerical solution via a finite element method applied to the full problem and for the value $K_c = 0.0084\,cm/day$.

Case of $\alpha(\tau) \neq 0$. If we assume that $a(\tau) \neq 0$ we have again the previous set of equations, (2.7), (2.8), and (2.10), with the difference that instead of equation (2.9) at $x = 0$, we have at $x = a(t)$, boundary conditions having the form

$$u(a(t),t) = \lambda_1, \quad v(a(t),t) = \lambda_2, \quad u(a(t),t) = \lambda_3,$$

and also an additional equation for the evolution of $a(t)$ is added (see [4]), i.e.

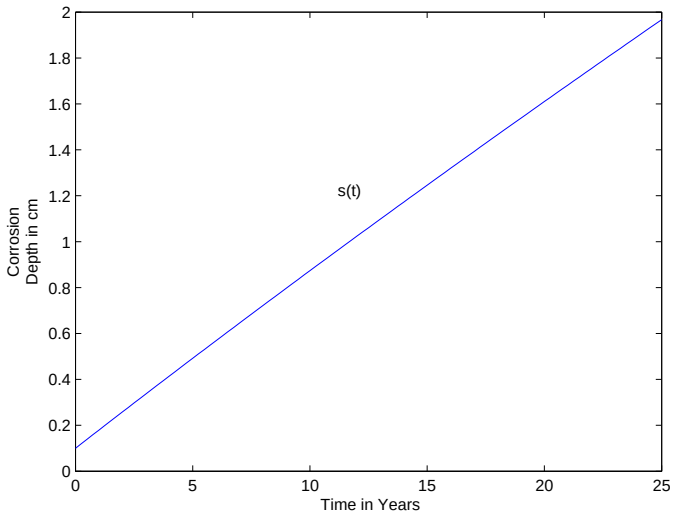

Fig. 2. *The free boundary, $s(t) = lS(\tau)$, plotted against time, arising by the numerical solution of problem (2.15) for $\gamma = 6.78$, $\beta_3 = 2.57 \cdot 10^{-2}$, $\nu_2 = 0.6313$, $s(0) = 0.1\,cm$. The length scale used here was $l = 2\,cm$.*

$$\dot{a}(t) = \left(1 - \frac{\rho_c}{\rho_g}\right) \frac{K_c}{C_c} w(s(t), t).$$

Scaling the equations in a similar way we get again the set of equations (2.7)-(2.10) but with $\alpha(\tau) < y < S(\tau)$, $\alpha(0) = 0$, where $\alpha = \frac{a}{l}$, and

$$\begin{aligned} U(\alpha(\tau), \tau) &= 1, \qquad & U_y(S(\tau), \tau) &= 0, \\ V(\alpha(\tau), \tau) &= 1, \qquad & V_y(S(\tau), \tau) &= 0, \\ W(\alpha(\tau), \tau) &= 1, \qquad & \gamma W_y(S(\tau), \tau) + W(S(\tau), \tau) &= 0. \end{aligned}$$

Also the equation for α (or for α_0 to leading order terms, if we consider a perturbation expansion of the form $\alpha = \alpha_0 + \epsilon\alpha_1 + \ldots$) becomes

$$\dot{\alpha}(\tau) = \gamma_a W(S(\tau), \tau),$$

where $\gamma_a = \left(1 - \frac{\rho_c}{\rho_g}\right)\left(\frac{t_0 K_c \lambda_3}{l C_c}\right)$, or $\gamma_a = \left(1 - \frac{\rho_c}{\rho_g}\right)$ given that $t_0 = \frac{l C_c}{K_c \lambda_3}$.

Following the same steps as before we have for U_0

$$U_{0yy} - \nu_2 U_0 = 0,$$
$$U(\alpha_0(\tau), \tau) = 1,\ U_y(S_0(\tau), \tau) = 0.$$

This results in the expression, for $U_0 \simeq V_0$,

$$U_0(y, \tau) = U_0(y;\, S_0(\tau)) = \frac{\cosh\left(\sqrt{\nu_2}(S_0(\tau) - y)\right)}{\cosh\left(\sqrt{\nu_2}(\alpha_0(\tau) - S_0(\tau))\right)}.$$

In addition W_0 which satisfies the equation

$$W_{0yy} - \beta_3 V_0 = 0,$$
$$W_0(\alpha_0(\tau), \tau) = 1, \qquad \gamma W_{0_y}(S_0(\tau), \tau) + W_0(S_0(\tau), \tau) = 0,$$

has the form

$$W_0(y, \tau) = \frac{(\beta_3 + \nu_2)\,(\gamma + S_0(\tau) - y)}{\nu_2\,(\gamma + S_0(\tau) - \alpha_0(\tau))} + \frac{\beta_3}{\nu_2\,(\gamma + S_0(\tau) - \alpha_0(\tau))}\,[y - \alpha_0(\tau)$$
$$-(\gamma + S_0(\tau) - \alpha_0(\tau))\cosh\left(\sqrt{\nu_2}(S_0(\tau) - y)\right)\operatorname{sech}\left(\sqrt{\nu_2}(\alpha_0(\tau) - S_0(\tau))\right)]\,. \quad (2.16)$$

Also

$$W_0(S(\tau), \tau) = \frac{\gamma}{\nu_2\,(\gamma + S_0(\tau) - \alpha_0(\tau))}\,[\beta_3 + \nu_2 - \beta_3 \operatorname{sech}\left(\sqrt{\nu_2}(\alpha_0(\tau) - S_0(\tau))\right)]\,.$$

Thus the equation for the free boundaries S and α, to leading order terms, now become

$$\frac{dS(\tau)}{d\tau} = \frac{\gamma}{\nu_2\,(\gamma + S(\tau) - \alpha(\tau))}\,[\beta_3 + \nu_2 - \beta_3 \operatorname{sech}\left(\sqrt{\nu_2}(\alpha(\tau) - S(\tau))\right)]\,, \quad (2.17a)$$

$$\frac{d\alpha(\tau)}{d\tau} = \frac{\gamma_a \gamma}{\nu_2\,(\gamma + S(\tau) - \alpha(\tau))}\,[\beta_3 + \nu_2 - \beta_3 \operatorname{sech}\left(\sqrt{\nu_2}(\alpha(\tau) - S(\tau))\right)]\,. \quad (2.17b)$$

In the following in Figure (3) we can see a simulation for $s(t) = S(\tau)l$ and $a(t) = \alpha(\tau)l$ against time, t, given by the solution of equations (2.17a, 2.17b). The expansion of the outer surface given by $a(t)$ is quite smaller compared with the magnitude of $s(t)$ due to the fact that $\gamma_a = -0.291$.

This result together with the numerical simulations in [4] can give us an overview of the behaviour of the solution of this model and its variations.

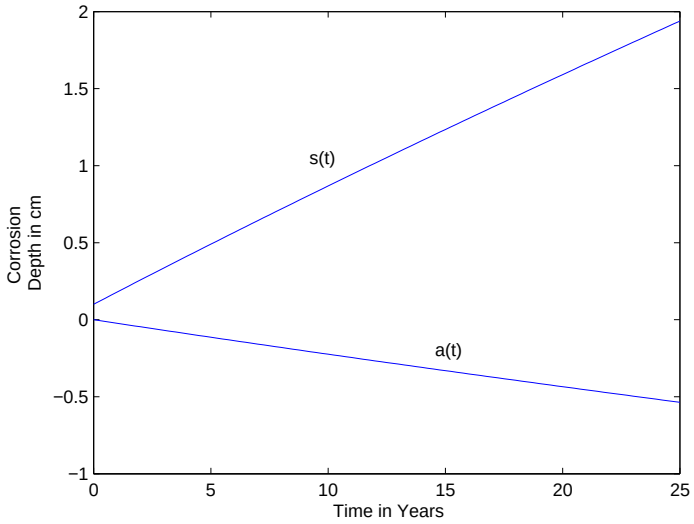

Fig. 3. *The free boundaries,* $s(t) = lS(\tau)$*, and* $a(t) = l\alpha(\tau)$ *are plotted against time using the numerical solution of equations (2.17) and for values of the parameters being the same as in Figure (2). Additionally* $\gamma_a = -0.291$*.*

Although this model assumes that there is a distinct interface between the corroded and the uncorroded part of the material. In order to make it more realistic it would be useful to construct a model which takes into account the formation of a region which is only partly corroded at times. This will be the subject of the next section.

3 Models for the Formation of a Mushy Region

As it is stated in [4] one could consider a model for the formation of gypsum which allows for gypsum and concrete to coexist at some volume element during the process.

In order to address this consideration we will assume that through the concrete and due to its porosity and the cracks existing in it, there is diffusion of H_2SO_4 which reacts with the concrete, i.e. the calcite, forming gypsum. The reaction takes place initially at the cracks' inner surface. Then gypsum is formed, having larger porosity than the concrete and thus new cracks are formed and diffusion takes place in the gypsum - vacuum (due to cracks) area. Based on this assumption in the following, we may take a specific element in the microstructure, actually determined by the space between neighbouring cracks, to be corroded in such a way, amongst possible others, so that the corrosion evolves in one - dimensional or two - dimensional way. Of course more complex approaches for the corrosion evolution in the microstructure can be taken leading to more complicated and possible more realistic mod-

els. Although the basic qualitative characteristics of the models of these kind should be apparent by the microstructure considerations presented here.

Note also that due to the difference in the densities of the calcite and the gypsum we may have an expansion of overall volume of the system. To keep things simple we will assume in the following of this work that this volume expansion is negligible and will not be further considered.

3.1 A One - Dimensional Model

Initially we will adopt a one - dimensional consideration regarding the geometry of the porous medium in the microstructure. We assume that it consists of material, $CaCO_3$, containing long-narrow cylindrical cracks, equispaced, and parallel between them. This assumption simplifies significantly the analysis that follows and we have to note that typical crack formations in concrete, (see e.g. [6], [7], [11]) indicate that the above assumption can be taken as a plausible first step to construct a fairly realistic model. Moreover note that we may consider a large in number set of pores and an additional one intersecting each one of them, so that to allow diffusion of liquid in the system. Near the cross sections of the pores we will have a certain behaviour during the process of corrosion which differs from the behaviour observed away from the intersections between the parallel pores. For simplicity reasons the behaviour near the intersections will not be taken into account in the models derived in the following. More specifically we will assume that the evolution of corrosion near the cross section of the pores does not effect significantly the overall process and in this work we will study only the corrosion process of pores which are parallel to each other. This consideration also accounts for the two - dimensional model derived in the next section.

We also assume that the distance between the cracks is $2d$. This length between two cracks can be taken to be the average distance between the axis of two parallel pores of cylindrical shape, in the material. A one - dimensional consideration can be seen in Figure (4).

Then in order to give some generality to our model we assume that H_2SO_4 diffuses in a one - dimensional way, in the direction perpendicular to the axis of the water filled cylindrical cracks (Figure (4)), or at the pores of the gypsum and its concentration satisfies the equation

$$\varepsilon W_\tau = W_{yy} + f(y, \tau),$$

Here ε is a parameter possible small for a suitable time scale, $W = W(y, \tau)$

again is the dimensionless concentration of H_2SO_4, y the dimensionless space variable ($y = \frac{x}{l}$ for x the dimensional space variable and l being a typical macroscopic length), τ the dimensionless time and f is some source term. In the pipe corrosion example f is $\beta_3 V(y,\tau)$ and ε corresponds to ϵ_3.

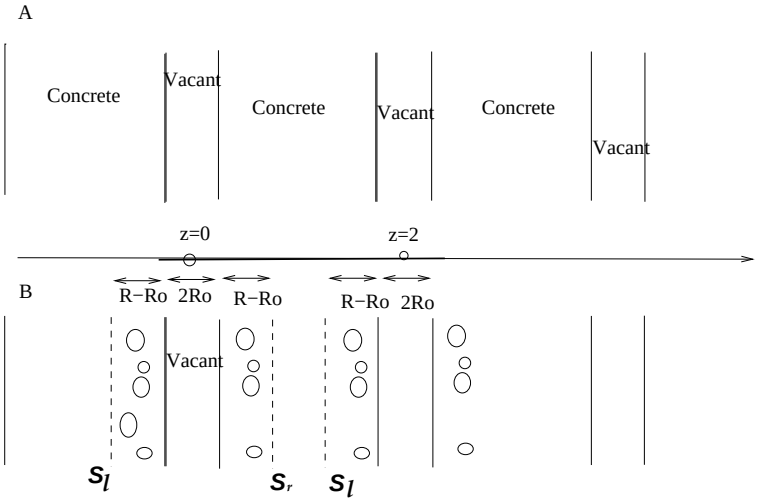

Fig. 4. *Schematic representation of one - dimensional considerations regarding the microstructure of the concrete*

Also at the crack surface we assume that we have flow of H_2SO_4 supplying the reaction at a rate proportional to W. More specifically we may have moving boundaries evolving to the right from the centre of the pore or to the left. Therefore the boundary conditions at the reaction front, for this one - dimensional geometry will have a form of Robin type

$$\pm\gamma W_y(y,\tau) + W(y,\tau) = 0,$$

for some constant $\gamma > 0$ and for (y,τ) a point in the boundary with the plus and minus sign taken when the boundary moves to the right or to the left respectively.

In addition the microscopic boundary moves, in each direction with speed σ being proportional to the rate of reaction so that at a point (y,τ) of a boundary we have

$$\sigma = W(y,\tau).$$

In the following we apply the methodology of the works [13] and [14]. We will consider two scales for the problem, the macroscopic length scale represented

by the variable y and a microscopic length scale represented by the variable z. As it is already mentioned l is a typical macroscopic length, say the width of a concrete slab or the thickness of a wall etc., whose corrosion is being studied and in addition we consider $2d$ to be the distance between the centre of two parallel pores of the material. Note that $d \ll l$. As a next step we take

$$W = W(y, z, \tau),$$

where $x = ly$ and $x = dz$ with $\delta = \frac{d}{l} \ll 1$. In addition we scale the dimensional position of the boundary, say s, with d, i.e. $S = \frac{s}{d}$ where S is the dimensionless position of the moving boundary and we make an appropriate choice of the time scale so that to balance the terms in the Stefan condition, e.g. in the pipe corrosion example we take now $t_0 = \frac{C_c d}{K_c \lambda_3}$. Moreover motivated by the form of the corresponding constant in equation (2.8c) we have $\gamma = \frac{D_H}{K_c l} = \frac{dD_H}{K_c l^2}\frac{l}{d} = \gamma_m \frac{1}{\delta}$, for $\gamma_m = \frac{dD_H}{K_c l^2}$. Thus in the following we will set $\gamma = \gamma_m \frac{1}{\delta}$ and we will assume that $\gamma_m = O(1)$.

The multiple scales approach gives instead for the spatial derivative $\frac{\partial W}{\partial y}$ at a point (y, z, τ), the expression

$$\frac{\partial W}{\partial y} + \frac{1}{\delta}\frac{\partial W}{\partial z},$$

and the equation for $W = W(y, z, \tau)$ will be

$$\varepsilon W_\tau = W_{yy} + \frac{1}{\delta^2} W_{yy} + f.$$

Also at the moving boundaries where $z = S$, the one moving to the left $S = S_l$ and the one moving to the right $S = S_r$, we have the boundary condition of Robin type which now becomes

$$\pm\gamma_m \frac{1}{\delta}\left(W_y(y, S, \tau) + \frac{1}{\delta}\frac{\partial W}{\partial z}(y, S, \tau)\right) + W(y, S, \tau) = 0.$$

Finally the Stefan condition, at the points (y, S, τ), $S = S_r$, S_l, and for a choice of the appropriate time scale, takes the form

$$\pm\frac{dS}{d\tau} = W(y, S, \tau),$$

where the plus sign accounts for $S = S_r$, increasing and the minus for $S = S_l$ decreasing. Also the width of the pores initially is equal to R_0 (see Figure (4 A)). As it is already stated the corrosion process evolves and two free boundaries appear. We set the centre of one pore to be taken at $z = 0$ while the centre of the parallel pore (with the same initial width) can be set at $z = 2$ and we take one front having distance R from $z = 0$, $S_r = R \geq R_0$ and moving to the right and the other, S_l, moving to the left and due to symmetry, having similarly, distance R from the point $z = 2$, i.e. $S_l = 2 - R$ (see Figure (4 B)). This means that the dimensionless width of the remaining concrete is $2 - 2R$, while the dimensionless width of the vacant - gypsum system is $2R$. Note that for $S = S_r$ by the Stefan condition and the Robin condition applied we take $\frac{dS_r}{d\tau} = -\frac{1}{\delta}\gamma_m(W_y + \frac{1}{\delta}W_z)$ while for $S = S_l$ similarly $-\frac{dS_l}{d\tau} = W = \frac{1}{\delta}\gamma_m(W_y + \frac{1}{\delta}W_z)$ and in both cases $\delta\frac{dS}{d\tau} = -\gamma_m(W_y + \frac{1}{\delta}W_z)$.

In addition due to the fact that we have infinite amount of pores parallel to each other which are undistinguished we may consider periodic conditions at the ends of an interval determined by the centres of two parallel pores, $z = 0$ and $z = 2$ and which is representative of the structure of the material. Hence we set periodic conditions at the boundary of the interval $[0, 2]$, i.e.

$$[W]_0^2 = 0, \quad [W_z + \delta W_y]_0^2 = 0.$$

Therefore, by assuming that the source term can be written in the form

$$f(y, \tau) = f_0(y, \tau) + \delta f_1(y, \tau) + \ldots,$$

and that $W \sim W_0 + \delta W_1 + \ldots$, the basic field equation, at the points (y, z, τ) with $z \in \Omega_g := [0, R] \cup [2 - R, 2]$, takes the form

$$\begin{aligned}\varepsilon W_{0\tau} + \varepsilon\delta W_{1\tau} + \varepsilon\delta^2 W_{2\tau} + \ldots = &\frac{1}{\delta^2}W_{0zz} + \frac{2}{\delta}W_{0zy} + W_{0yy} + f_0\\ &+\frac{1}{\delta}W_{1zz} + 2W_{1zy} + \delta W_{1yy} + \delta f_1\\ &+W_{2zz} + 2\delta W_{2zy} + \delta^2 W_{2yy} + \delta^2 f_2\\ &+\delta W_{3zz} + 2\delta^2 W_{3zy} + \ldots.\end{aligned}$$

At the free boundaries formed during corrosion $S = S_r$, S_l, we have for $S \sim S_0 + \delta S_1 + \ldots$, and $W(y, S_0 + \delta\, S_1 + \ldots, \tau) \sim W(y, S_0, \tau) + \delta\, S_1 W_z(y, S_0, \tau) + \ldots$, that

$$\pm\gamma_m\left(\frac{1}{\delta^2}W_{0z}+\frac{1}{\delta}W_{0y}+\frac{1}{\delta}W_{1z}+W_{1y}+W_{2z}+\frac{1}{\delta}S_1W_{0zz}+S_1W_{0yz}+S_1W_{1zz}+\ldots\right)$$
$$+W_0+\delta W_1+\delta S_1W_{0z}+\ldots=0,$$

at the points (y, S_0, τ).

In addition the free boundary condition at the same points will become

$$\frac{dS_0}{d\tau}+\delta\frac{dS_1}{d\tau}+\ldots=-\gamma_m\left(\frac{1}{\delta^2}W_{0z}+\frac{1}{\delta}W_{0y}+\frac{1}{\delta}W_{1z}+W_{1y}+W_{2z}+\delta W_{2y}+\delta W_{3z}\right.$$
$$\left.+\frac{1}{\delta}S_1W_{0zz}+S_1W_{0yz}+S_1W_{1zz}+\ldots\right).$$

Similarly the periodic conditions at $z = 0, 2$, have the form

$$\left[\frac{1}{\delta^2}W_0+\frac{1}{\delta}W_1+W_2+\ldots\right]_{z=0}^{z=2}=0,$$

and

$$\left[\frac{1}{\delta^2}W_{0z}+\frac{1}{\delta}W_{0y}+\frac{1}{\delta}W_{1z}+W_{1y}+W_{2z}+\ldots\right]_{z=0}^{z=2}=0.$$

Equating $O(\frac{1}{\delta^2})$ terms we obtain

$$W_{0zz}=0,$$

at the points (y, z, τ) with $z \in \Omega_g$, while by the periodic conditions at $z = 0, 2$ we have

$$[W_{0z}]_{z=0}^{z=2}=0, \quad [W_0]_{z=0}^{z=2}=0.$$

Also at $z = S = S_r$, $S_l \sim S_0$ we have

$$W_{0z}=0.$$

The above equations implies that $W_{0z}(y,z,\tau) = 0$ and consequently that $W_0 = W_0(y,\tau)$.

For the $O(\frac{1}{\delta})$ terms similarly, given that $W_0 = W_0(y,\tau)$, we have

$$W_{1zz} = 0,$$

at the points (y,z,τ) with $z \in \Omega_g$, with the relevant periodic conditions at $z = 0$, 2 being $\left[W_{0y} + W_{1z}\right]_{z=0}^{z=2} = 0$ and $[W_1]_{z=0}^{z=2} = 0$. Also at $z = S = S_r$, $S_l \sim S_0$ we have $W_{0y} + W_{1z} = 0$, to leading order terms. Therefore again as for W_0 we deduce that $W_{1z} = 0$ or that $W_1 = W_1(y,\tau)$.

Continuing for $O(1)$ terms, and for $z \in \Omega_g$, we have

$$\varepsilon W_{0\tau} = W_{0yy} + W_{2zz} + f_0, \tag{3.1}$$

with the conditions

$$[W_2]_{z=0}^{z=2} = 0, \quad \left[W_{1y} + W_{2z}\right]_{z=0}^{z=2} = 0,$$

at the points $(y,0,\tau)$, $(y,2,\tau)$, and

$$\pm\gamma_m(W_{1y} + W_{2z}) + W_0 = 0,$$

at $z = S = S_r$, $S_l \sim S_0$. In addition the equation for S will give

$$\frac{dS_0(\tau)}{d\tau} = -\gamma_m \left(W_{1y} + W_{2z}\right)$$

at $z = S = S_r, S_l \sim S_0$ to leading order terms.

Averaging equation (3.1) over z will result, due to the periodic conditions applied at the ends of the interval $[0,2]$, in the equation,

$$\int_0^{S_r} + \int_{S_l}^2 \left[\varepsilon W_{0\tau} - W_{0yy}\right] dz = \int_0^{S_r} + \int_{S_l}^2 f_0(y,\tau)dz + W_{2z}|_{z=2} - W_{2z}|_{z=S_l} + W_{2z}|_{z=S_r} - W_{2z}|_{z=0}.$$

Due to the periodic conditions $[W_2]_{z=0}^{z=2} = 0$ and $\left[W_{1y} + W_{2z}\right]_{z=0}^{z=2} = 0$, the condition for the free boundary

$$[W_{2z}]_{z=S_r} = -\frac{1}{\gamma_m}\frac{dS_r(\tau)}{d\tau} - \left[W_{1y}\right]_{z=S_r},$$

$$[W_{2z}]_{z=S_l} = -\frac{1}{\gamma_m}\frac{dS_l(\tau)}{d\tau} - \left[W_{1y}\right]_{z=S_l},$$

and the fact that $W_1 = W_1(y,\tau)$ which implies that W_1 does not vary significantly over $z \in [0,2]$ giving $[W_{1y}]_{z=0}^{z=2} = 0$, $[W_{1y}]_{z=S_r}^{z=S_l} = 0$, we obtain finally, for ϕ_g being the constant gypsum porosity and for $S_l = 2 - R$, $S_r = R$, that

$$\begin{aligned} 2R\phi_g\left[\varepsilon W_{0\tau} - W_{0yy} - f_0(y,\tau)\right] &= \frac{1}{\gamma_m}\left(-\frac{dS_r(\tau)}{d\tau} + \frac{dS_l(\tau)}{d\tau}\right) \\ &= \frac{1}{\gamma_m}\left(-\frac{\partial R}{\partial \tau} + \frac{\partial(2-R)}{\partial \tau}\right) = -\frac{2}{\gamma_m}\frac{\partial R}{\partial \tau}. \end{aligned}$$

By denoting with W the dominant term W_0 we have the macroscopic equation

$$\varepsilon W_\tau = W_{yy} + f_0(y,\tau) - \frac{1}{\gamma_m \phi_g R}\frac{\partial R}{\partial \tau}, \tag{3.2}$$

with

$$\frac{\partial R}{\partial \tau} = \begin{cases} 0, & R = R_0 \text{ and } \tau < \tau_1(y), \text{ or } R = 1 \text{ and } \tau > \tau_2(y), \\ W(y,\tau), & R_0 < R < 1, \end{cases} \tag{3.3}$$

and $R(y,0) = R_0$. The time $\tau_1(y)$ denotes the time when $W(y,\tau)$ becomes positive for the first time at the point y and $\tau_2(y)$ denotes the time when R reaches one at the same point. For $W(y,\tau) > 0$, R increases starting from R_0 till it reaches the value $R = 1$. Note also that R should depend only on the time τ and the macroscopic position y, $R = R(y,\tau)$ as it is also emerge from equation (3.3).

This equation applies for the actual concentration W of a substance contained in the water inside the pores of the material. In order to measure the effective

concentration we take this to be $\bar{W} = \phi W$, where $\phi = \phi(y, \tau)$ is the porosity of the material corresponding to the interval [0, 2] i.e. the ratio of vacant over the total volume of the material in $[0, 2]$. When the whole of the material in the interval $[0, 2]$ is uncorroded we have $\phi = \phi_c$ and the initial radius of the pore is fixed so that $R_0 = \phi_c$, while when it is fully corroded $\phi = \phi_g$. Hence we have $\phi_c < \phi < \phi_g$, for ϕ depending directly from $R = R(y, \tau)$ via the relation $\phi(y, \tau) = \phi(R(y, \tau)) = \frac{(R(y,\tau)+\phi_b)}{\phi_a}$, where $\phi_a = \frac{1-\phi_c}{\phi_g-\phi_c}$ and $\phi_b = \frac{\phi_c(1-\phi_g)}{\phi_g-\phi_c}$ are appropriate constants giving $\phi(R_0) = \phi_c$ and $\phi(1) = \phi_g$.

Therefore the system of equations (3.2) and (3.3) with appropriate boundary and initial conditions form a phase field model for concrete corrosion. Up to this point we have considered the gypsum evolving in a one - dimensional direction and actually taking as an element characterizing the microstructure of the material the interval $[0, 2d]$. We can continue with a more realistic approach by considering instead such a microscopic element to be a square, with side $2d$ and having at its four corners pores of radius R_0 centered at the vertexes of this square (see Figure (5)).

3.2 A Two - Dimensional Model

Again we consider the equation

$$\varepsilon W_\tau = \Delta W + f(y, \tau),$$

with f being the source term and $y = (y_1, y_2)$. The diffusion takes place now in two spatial dimensions. In addition the boundary condition at the interface Γ of the corroded - uncorroded material will be

$$\gamma_m \frac{1}{\delta} \frac{\partial W}{\partial n} + W = 0, \quad y \in \Gamma,$$

where n is the outward normal vector at a point of the moving boundary Γ, while the motion of the boundary is given by the standard Stefan condition

$$-\gamma_m \frac{\partial W}{\partial n} = \sigma, \quad y \in \Gamma$$

where σ is the speed of the moving boundary. The latter comes from the fact, as in the one - dimensional case, that the speed of the moving boundary Γ is

proportional to the rate of reaction, $\sigma = W$ and the Robin condition taken there.

Regarding the geometry of the porous medium we assume, as in the previous section, that it consists of matter containing cracks parallel between them and that the average distance between the axes of these cracks is of length $2d$ (see Figure (5)). Also the relevant scale for the macroscopic problem is taken again to be l. In addition we will take the variation of the concentration of

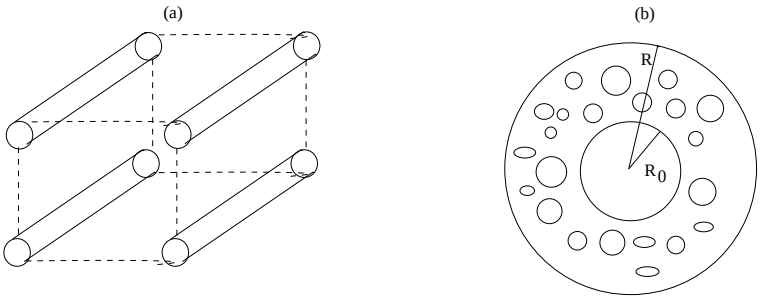

Fig. 5. *Schematic representation of a three - dimensional considerations regarding the microstructure of the concrete*

H_2SO_4 in the axial direction of the crack to be negligible, or equivalently the length of the cylindrical crack to be much larger than the distance between the axes of the cracks which is $2d$. Thus actually we have a two - dimensional consideration of the microscale model.

For the pores that are of cylindrical shape, we take the initial pore radius to be R_0. When the reaction takes place gypsum is formed and more cracks appear in which diffusion takes place, till the whole element is transformed to gypsum with porosity ϕ_g.

Now we scale distance in the usual way, i.e. $x = ly$ and $x = dz$, with $y = (y_1, y_2)$, $z = (z_1, z_2)$, $y = \frac{d}{l}z$ with $\frac{d}{l} \ll 1$. The porosity of the calcite is ϕ_c, constant and we must have $\frac{\pi R_0^2}{4} = \phi_c$ or the value of R_0 to be fixed by the relation $R_0 = 2\left(\frac{\phi_c}{\pi}\right)^{\frac{1}{2}}$. Note also that we may assume, when this is convenient, radially symmetry in the $y_1 - y_2$ plane. Application of the multiple scales method implies

$$\varepsilon W_\tau = \frac{1}{\delta^2}\nabla_z^2 W + \frac{2}{\delta}\nabla_y\nabla_z W + \nabla_y^2 W + f(y,\tau).$$

Regarding the condition at the moving boundary, due to the radial symmetry assumption already imposed, we will assume that the moving boundary Γ has form of a circular arc of radius R and that its speed is proportional to the variation of the radius with respect to time, $\frac{\partial R}{\partial \tau}$. In conclusion at the boundary Γ where $|z| = R = R(y,z,\tau)$ or $z_1^2 + z_2^2 = R^2$ for $(z_1, z_2) \in \Gamma$, after appropriate scaling, as we did in the one - dimensional case we will have

$$\delta^2 \frac{\partial R}{\partial \tau} = -\gamma_m \, n \cdot \left[\nabla_z W + \delta \nabla_y W\right],$$

and

$$\gamma_m \, n \cdot \left[\nabla_z W + \delta \nabla_y W\right] + \delta^2 W = 0.$$

Note that as it is already mentioned the centres of four parallel neighbouring circular intersections of the pores form a square of side $2d$. The boundary of this square is taken to be the outer boundary of an element of the material which is to be studied, denoted by $\Omega := [0,\,2] \times [0,\,2]$, $z \in \Omega$ and in which symmetry conditions should be applied for the variable W. We will apply periodic conditions at the sides of the square boundary of the following form:

$$\begin{aligned}
W(y, z_1, 0, \tau) &= W(y, z_1, 2, \tau), \quad 0 \le z_1 \le 2,\\
W(y, 0, z_2, \tau) &= W(y, 2, z_2, \tau), \quad 0 \le z_2 \le 2,\\
W_{z_2}(y, z_1, 0, \tau) &= W_{z_2}(y, z_1, 2, \tau), \quad 0 \le z_1 \le 2,\\
W_{z_1}(y, 0, z_2, \tau) &= W_{z_1}(y, 2, z_2, \tau), \quad 0 \le z_2 \le 2,
\end{aligned}$$

or summarizing the above relations $\nabla W|_{\partial\Omega} = 0$. In a similar way as in the one - dimensional case this condition also expresses the fact that we consider an infinite set of square cells, inside the material indistinguishable between them and therefore periodic condition should be applied in the outer boundary of them. Thus for the rest of our analysis we focus our attention in one cell occupying a region Ω with boundary $\partial\Omega$.

The equations for W, by assuming that $W \sim W_0 + \varepsilon W_1 + \ldots$, will take the form

$$\begin{aligned}\varepsilon W_{0\tau}+\delta\varepsilon W_{1\tau}+\delta^2\varepsilon W_{2\tau}+\ldots=&\frac{1}{\delta^2}\nabla_z^2W_0+\frac{2}{\delta}\nabla_z\nabla_yW_0+\nabla_y^2W_0+f_0\\&+\frac{1}{\delta}\nabla_z^2W_1+2\nabla_z\nabla_yW_1+\delta\nabla_y^2W_1+\delta f_1\\&+\nabla_z^2W_2+2\delta\nabla_z\nabla_yW_2+\delta^2\nabla_y^2W_2+\delta^2f_2\\&+\delta\nabla_z^2W_3+2\delta^2\nabla_z\nabla_yW_3+\ldots.\end{aligned}$$

Also at the points (y,z,τ) with $z=(z_1,z_2)\in\Gamma$, we have that

$$\begin{aligned}\frac{\partial R}{\partial\tau}&=-\gamma_m\,n\cdot\left[\frac{1}{\delta^2}\nabla_zW_0+\frac{1}{\delta}\nabla_yW_0+\frac{1}{\delta}\nabla_zW_1+\nabla_yW_1+\nabla_zW_2+\ldots\right],\\W_0+\ldots+\gamma_m\,n\cdot&\left[\frac{1}{\delta^2}\nabla_zW_0+\frac{1}{\delta}\nabla_yW_0+\frac{1}{\delta}\nabla_zW_1+\nabla_yW_1+\nabla_zW_2+\ldots\right]=0.\end{aligned}$$

Then for order $O(\frac{1}{\delta^2})$ terms we have $\nabla_z^2W_0=0$. By the conditions at the moving boundary Γ, i.e. at $z=R$ we get $n\cdot\nabla_zW_0=0$. In addition at the cell boundary, $\partial\Omega$ we have again $n\cdot\nabla_zW_0=0$. By these equations and a direct application of the maximum principle we deduce that $W_0=W_0(y,\tau)$.

For order $O(\frac{1}{\delta})$ terms we have $2\nabla_z\nabla_yW_0+\nabla_z^2W_1=0$, or $\nabla_z^2W_1=0$ due to the fact that $W_0=W_0(y,\tau)$. In addition at $z=R$ we have $n\cdot[\nabla_yW_0+\nabla_zW_1]=0$ while at the cell boundary, $\partial\Omega$ we have similarly $n\cdot[\nabla_yW_0+\nabla_zW_1]=0$. As for the $O(\frac{1}{\delta^2})$ terms by using the same arguments and the fact that $n\cdot\nabla_yW_0=0$ over the boundary because W_0 does not vary significantly in the $z-$scale, we deduce that $W_1=W_1(y,\tau)$.

For $O(1)$ terms, given that $\nabla_zW_1=0$, we have

$$\varepsilon W_{0\tau}=\nabla_y^2W_0+\nabla_z^2W_2+f_0(y,\tau),$$

while at $z=R$,

$$\frac{\partial R}{\partial\tau}=-\gamma_m\,n\cdot\left[\nabla_yW_1+\nabla_zW_2\right].$$

As for the one - dimensional case we may proceed by averaging the field equation over the whole domain occupied by the gypsum or vacants, say Ω_g. Due

to the fact that periodic conditions are applied to each of the indistinguishable cells averaging of the equation for W_0 will result in the following equation:

$$\int_{\Omega_g} \left[\varepsilon W_{0\tau} - \nabla_y^2 W_0 - f_0(y,\tau)\right] dz = \int_{\Omega_g} \nabla_z^2 W_2 dz = \int_{\Gamma\cup\Gamma_e} n\cdot\nabla_z W_2 dz,$$

for $\Gamma_e = \partial\Omega \bigcap \partial\Omega_g$, or

$$\phi_g A(R) \left[\varepsilon W_{0\tau} - \nabla_y^2 W_0 - f_0(y,\tau)\right] = \int_{\Gamma} n\cdot\nabla_z W_2 dz + \int_{\Gamma_e} n\cdot\nabla_z W_2 dz,$$

where $A(R)$ is the area of the cell occupied by the gypsum. Note that the

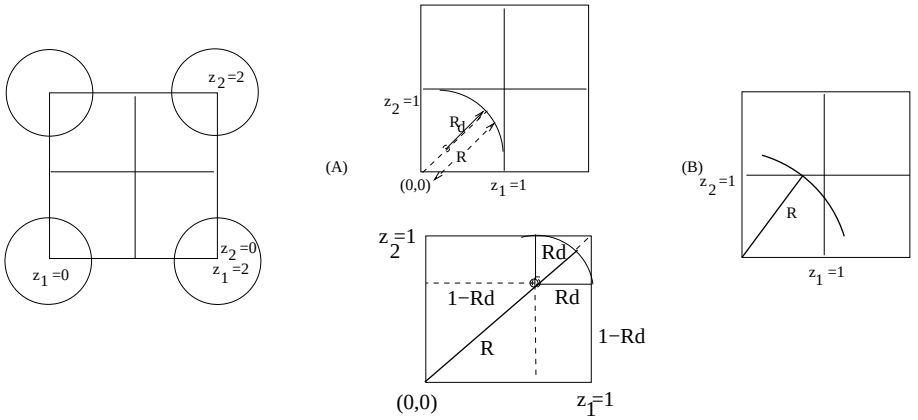

Fig. 6. *Schematic representation of configurations A and B*

symmetry conditions at the cell boundary $\partial\Omega$ gives $\int_{\Gamma_e} n\cdot\nabla_z W_2 dz = 0$ and we also have $\int_{\Gamma\cup\Gamma_e} n\cdot\nabla_y W_1 dz = 0$. Now we denote by $F(R)$ the source term appearing in the equation of W_0,

$$F(R) := \int_{\Gamma\cup\Gamma_e} n\cdot\nabla_z W_2 dz = -\frac{1}{\gamma_m}\frac{\partial R}{\partial\tau}\int_{\Gamma} dz.$$

In the case that $R_0 \le R \le 1$ we have that $\int_\Gamma dz = 2\pi R$ while the relevant area is $A(R) = \pi R^2$.

In the case that $1 \le R \le \sqrt{2}$ we may have two configurations. In general by the behaviour of free boundary problems of such kind and due to the symmetry of the problem, we expect in our case to have a moving boundary with the shape of a circular arc. Consequently depending the way that the boundary

intersects with the lines $z_1 = 1$, $0 \leq z_2 \leq 2$ or $z_2 = 1$, $0 \leq z_1 \leq 2$ inside the square element we may have two different configurations (see Figure (6)). We may assume that after the time the radius R exceeds one, the circular arc is tangent to these lines, or that it intersects them with its tangent at the intersection points, forming some angle with it (see also [13]).

Case A The boundary is a circle arc tangent to the lines $z_1 = 1$ and $z_2 = 1$. In this case the area of the gypsum in one of the quarters of the cell, $\Omega = [0,\, 2] \times [0,\, 2]$, will be the sum of three rectangles and a circular segment of radius R_d, where R_d is the radius of the circle which its circular arc is tangent to the lines $z_1 = 1$, $0 \leq z_2 \leq 2$ and $z_2 = 1$, $0 \leq z_1 \leq 2$. Thus the area occupied by the gypsum in this quarter will be $2R_d(1 - R_d) + (1 - R_d)^2 + \frac{\pi R_d^2}{4}$ and the area of the gypsum in the whole cell will be $A(R) = 4\left(1 - R_d^2(1 - \frac{\pi}{4})\right)$ (see Figure 6A). Also if R, measures the distance from the point of intersection of the circular arc and the line $z_2 = z_1$ to the point $(z_1, z_2) = (0, 0)$ we have that $(R - R_d) + \sqrt{2}R_d = \sqrt{2}$ or that $R_d = \frac{R - \sqrt{2}}{1 - \sqrt{2}}$. In addition the overall length of the arcs consisting the boundary Γ, is $L(R) = 2\pi R_d$.

In this case the field equation, by denoting with W the dominant term W_0, becomes

$$\varepsilon W_\tau = \nabla_y^2 W + f_0(y, \tau) + F(R), \tag{3.4}$$

with

$$F(R) = \begin{cases} -\frac{2}{\gamma_m \phi_g} \frac{1}{R} \frac{\partial R}{\partial \tau}, & R_0 \leq R \leq 1, \\ -\frac{\pi R_d}{2\gamma_m \phi_g \left[1 - R_d^2(1 - \frac{\pi}{4})\right]} \frac{\partial R}{\partial \tau}, & 1 < R \leq \sqrt{2}, \end{cases} \tag{3.5}$$

In addition to leading order terms, by the Robbin condition at the moving boundary Γ, $\gamma_m\, n \cdot \nabla W + W = 0$ we obtain the equation for macroscopic variable R which is

$$\frac{\partial R}{\partial \tau} = W(y, \tau). \tag{3.6}$$

Case B The boundary is a circle that has radius R and at all times intersects the lines $z_1 = 1$ and $z_2 = 1$ at some angle ϕ. In this case $L(R) =$

$2R\left[\pi - 4\cos^{-1}\left(\frac{1}{R}\right)\right]$ and $A(R) = 4\left[\sqrt{R^2-1} + \frac{R^2}{2}\left(\frac{\pi}{2} - 2\cos^{-1}\left(\frac{1}{R}\right)\right)\right]$. Then the field equation is again given by equation (3.4) and (3.6) but with

$$F(R) = \begin{cases} -\frac{2}{\gamma_m \phi_g}\frac{1}{R}\frac{\partial R}{\partial \tau}, & R_0 \leq R \leq 1, \\ -\frac{R\left[\pi - 4\cos^{-1}\left(\frac{1}{R}\right)\right]}{2\gamma_m\phi_g\left[\sqrt{R^2-1}+\frac{R^2}{4}\left(\pi-4\cos^{-1}\left(\frac{1}{R}\right)\right)\right]}\frac{\partial R}{\partial \tau}, & 1 < R \leq \sqrt{2}. \end{cases} \tag{3.7}$$

4 Numerical Solution

In order to obtain a numerical solution of the various phase field models derived in Section (3) we will use a finite element method, regarding space discretization, combined with the two step Crank- Nicholson method, indicating that the scheme is unconditionally stable.

Initially we will solve numerically the model given by equations (3.2) and (3.3). Note that as it is already mentioned these equations account for the actual concentration W of SO_4^{2-} while the effective concentration $\bar{W}$ is given by $\bar{W} = \phi W$, for ϕ being the porosity of the material, $\phi = \phi(y, \tau)$. In addition, given that $R(y, 0) = R_0 = \phi_c$ we have that $\phi = \phi_c + (R - \phi_c)\frac{(\phi_g - \phi_c)}{1-\phi_c}$ or that $R = \left(\frac{1-\phi_c}{\phi_g - \phi_c}\right)\phi - \phi_c\frac{1-\phi_c}{\phi_g-\phi_c}$ and $\frac{\partial R}{\partial \tau} = \left(\frac{1-\phi_c}{\phi_g-\phi_c}\right)\frac{\partial \phi}{\partial \tau}$. We will consider a uniform cement slab with $y \in [0, 1]$ (this may come after appropriate scaling) and we will also take no flux, Neumann condition at $y = 1$ corresponding to an assumption of symmetry. The latter may be the case when we examine a wall of dimensionless length 2 exposed in H_2SO_4 from both sides. Alternatively this no flux condition may result in the case where the right part of the wall is isolated. At $y = 0$ we assume that the effective concentration is equal to one.

Then the system of equations to be solved takes the form of equations (3.2) and (3.3) together with the following boundary and initial conditions

$$\phi(0, \tau)W(0, \tau) = 1, \quad \frac{\partial}{\partial y}\left(\phi(1, \tau)W(1, \tau)\right) = 0, \tag{4.1}$$

$$W(y, 0) = 0, \quad R(y, 0) = 0. \tag{4.2}$$

We discretize the system of equations in the following way. We consider a grid of the domain $[0, 1] \times [0, T]$, where T is the final time of a potential simulation. Regarding the interval $[0, 1]$ we take $M + 1$ points $y_j = j \cdot \delta y$ for δy being the spatial step for $j = 0, 1, 2, \cdots M$. In addition in the interval $[0, T]$ we take

N time steps of size $\delta\tau$, where $N = [T/\delta\tau]$ and with the points of the time discretization being $\tau_i = i\delta\tau$, $i = 1, 2, \ldots N$.

Let Φ_j, $j = 0, \ldots, M$ denote the standard linear B - splines on the interval [0, 1], defined with respect to the partition considered.

$$\Phi_j = \begin{cases} \frac{y-y_{j-1}}{\delta y}, & y_{j-1} \le y \le y_j, \\ \frac{y_{j+1}-y}{\delta y}, & y_j \le y \le y_{j+1}, \\ 0, \quad \text{elsewhere in} \quad [0,\, 1], \end{cases} \tag{4.3}$$

for $j = 0, 1, 2, \ldots, M$. We then set $W(y, \tau) = \sum_{j=0}^{M} a_{w_j}(\tau)\Phi_j(y)$, and $R(y, \tau) = \sum_{j=0}^{M} a_{R_j}(\tau)\Phi_j(y)$, $\tau \ge 0$, $0 \le y \le 1$.

Substituting these expressions for W and R into the relevant equations and applying the standard Galerkin method, i.e. multiplying with Φ_i, for $i = 1, 2, \ldots, M$ and integrating over [0, 1] we obtain a system of equations for the a_w's and the a_R's.

$$\varepsilon \sum_{j=0}^{M} \dot{a}_{w_j}(\tau) < \Phi_j(y)\, \Phi_i(y) > = -\sum_{j=0}^{M} a_{w_j}(\tau) < \Phi_j'(y)\, \Phi_i'(y) > + < F\left(\sum_{j=0}^{M} a_{R_j}(\tau)\Phi_j(y)\right) \Phi_i(y) >, \tag{4.4}$$

$$\dot{a}_{R_j}(\tau) = a_{w_j}(\tau), \tag{4.5}$$

where $< f, g > := \int_0^1 f(y)g(y)dy$ and $i = 1, 2, \ldots, M$. Setting $a_w = [a_{w_1},\, a_{w_2}, \ldots, a_{w_M}]^T$ and $a_R = [a_{R_1},\, a_{R_2}, \ldots, a_{R_M}]^T$ the system of equations for the a_w's and the a_R's take the form

$$\begin{aligned} A\dot{a}_w(\tau) &= -Ba_w(\tau) + b(\tau), \\ \dot{a}_R(\tau) &= a_w(\tau), \end{aligned}$$

where, taking also into account the boundary conditions, (4.1), and (4.2) the matrices A, B and b have the form

$$A = \varepsilon\delta y \begin{bmatrix} \frac{2}{3} & \frac{1}{6} & 0 & \dots & 0 \\ \frac{1}{6} & \frac{2}{3} & \frac{1}{6} & \dots & 0 \\ 0 & 0 & \ddots & \ddots & 0 \\ 0 & 0 & \dots & \frac{1}{6} & \frac{1}{3} \end{bmatrix}, \; B = \frac{1}{\delta y} \begin{bmatrix} 2 & -1 & 0 & \dots & 0 \\ -1 & 2 & -1 & \dots & 0 \\ 0 & 0 & \ddots & \ddots & 0 \\ 0 & 0 & \dots & -1 & \frac{\phi_y(1)}{\phi(1)} + 1 \end{bmatrix}, \; b(t) = \begin{bmatrix} \frac{1}{\phi(0)} + < F(R), \Phi_1 > \\ < F(R), \Phi_2 > \\ \vdots \\ < F(R), \Phi_M > \end{bmatrix}$$

We then apply the three time step approximation by taking $\dot{a}_w(\tau_n) \simeq \frac{a_w^{n+1} - a_w^{n-1}}{2\delta\tau}$. The relevant equation then becomes

$$A\left(\frac{a_w^{n+1} - a_w^{n-1}}{2\delta\tau}\right) = -B\left(\frac{a_w^{n+1} + a_w^{n-1}}{2}\right) + b^n,$$

where $b^n = b(t_n)$.

After some manipulation we obtain the equations

$$a_w^{n+1} = (A + \delta\tau B)^{-1}\left[(A - \delta\tau B)a_w^{n-1} + 2\delta\tau\, b^n\right], \tag{4.6a}$$

$$a_R^{n+1} = a_R^{n-1} + 2\delta\tau a_w^n. \tag{4.6b}$$

Note that for the second time step we have in place of equations (4.6).

$$a_w^2 = (A + \delta\tau B)^{-1}\left[(A - \delta\tau B)a_w^1 + \delta\tau\, b^1\right], \tag{4.7a}$$

$$a_R^2 = a_R^1 + \delta\tau a_w^1, \tag{4.7b}$$

for a_w^1 and a_R^1 being determined by the initial conditions.

In Figure (7) the system of equations (3.2) and (3.3) with the boundary and initial conditions (4.1) and (4.2), is solved numerically and the free boundaries given by the conditions $R(y,\tau) = R_0$ and $R(y,\tau) = 1$ (dotted line), are plotted against time. Also in the same Figure (7) the system of equations (3.2) and (3.3) with the same boundary conditions is solved numerically, in the case that configuration A (solid line) and B (dashed line) are considered, i.e. for source terms given by equations (3.5) and (3.6). For these cases the free boundaries given by the conditions $R(y,\tau) = R_0$ and $R(y,\tau) = \sqrt{2}$, are plotted against time. The lower boundaries coincide while the upper boundaries are distinctive indicating that in the case of configuration A the transition into gypsum takes place slower at the inner part of the material. Note also that in all of the above simulations the lower boundary is a line parallel to the spatial axis (some small variations are not visible in the Figure). This indicates that almost immediately, at $\tau = 0$, the whole of the material enters the mushy region and for all $y \in [0,1]$ the material is partly corroded with $R(y,\tau)$ exceeding R_0, for $\tau \geq 0$.

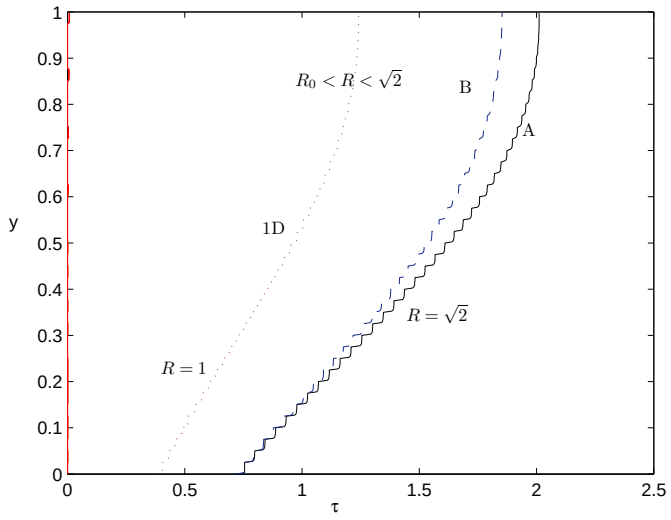

Fig. 7. *The free boundaries, given by the conditions* $R(\tau) = R_0$ *and* $R(\tau) = 1$, *are plotted against time after solving numerically the equations (3.2) and (3.3) with the relevant boundary conditions, for* $M = 61$, $\varepsilon = 1$, $\gamma_m = 1$, $\phi_c = 0.4$, $\phi_g = 0.6$ $\delta\tau = .8 * \delta y^2$.

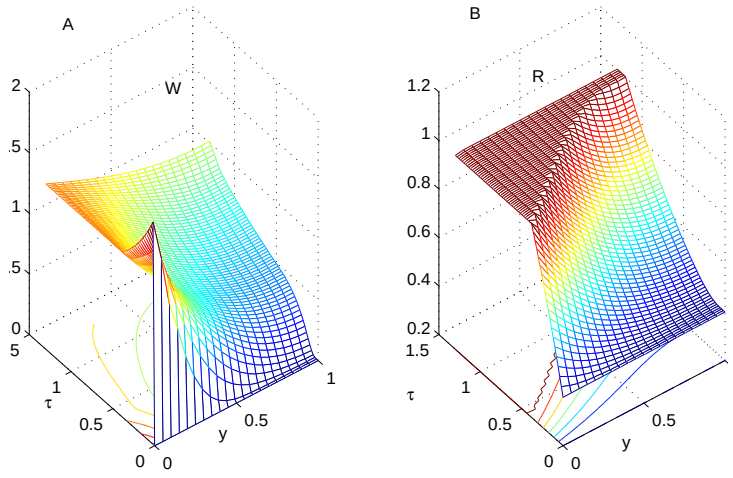

Fig. 8. *The concentration of sulfide,* W *and of the macroscopic parameter* R *are plotted against space* y *and time* τ *in the subfigures A and B respectively. These graphs are produced by the numerical solution of equations (3.2) and (3.3). The values of the parameters taken were* $M = 21$, $\varepsilon = 1$, $\delta_0 = 1$, $\phi_c = 0.4$, $\phi_g = 0.6$ $\delta\tau = 0.8 \cdot \delta y^2$.

Finally in Figure (8) the system of equations (3.2) and (3.3) with boundary and initial conditions (4.1) and (4.2) is solved numerically, in the case that we have the one - dimensional consideration. The form of W can be seen in Figure (8)A where it is plotted against space and time. Note that there is a variation in the value of W at $y = 0$ because of the change of the porosity.

In Figure (8)B the macroscopic variable R is plotted against space and time. The points where R reaches one indicate when this part of the material is fully transformed into gypsum.

Simulations in the case of sewer pipes corrosion Going back to the example of the sewer pipes corrosion we modify accordingly the equations of U, V and W so that to account for the formation of the mushy region. Applying the same procedure as in Section 3.2 we can derive the equations for U, V, W the same way that equation (3.2) or (3.4) has been derived.

The equations of dimensional variables corresponding to U, V and W have the same form as the system of equations (2.1), but with the difference that these variables now denote the actual concentration and not the effective concentration and that in the equation of W the sink term appears $\propto \frac{\partial R}{\partial \tau}$ representing the amount of W which is absorbed by the reaction during the process. The porosity ϕ, i.e. the ratio of vacant over the total volume of a cell of material, which consists of both calsite and gypsum, in the present one - dimensional case, is a variable and a function of space and time with $\phi_c < \phi < \phi_g$. We have $\phi = \phi_c$ when the cell under consideration is uncorroded and $\phi = \phi_g$ when the process of corrosion is complete. Also we have that, for the one - dimensional model consideration the porosity to be $\phi = \frac{1}{1-\phi_c}\left[(\phi_g - \phi_c)R + \phi_c(1-\phi_g)\right]$.

More specifically the form of the equation for the actual concentrations will be the same as equations (2.1) but with different diffusion coefficients.

$$u_t = D_{ha}u_{xx} - \frac{K_T A_S}{V_a}(K_{HS}u - v), \tag{4.8a}$$

$$v_t = D_{hw}v_{xx} + \frac{K_T A_S}{V_w}(K_{HS}u - v) - K_B v, \tag{4.8b}$$

$$w_t = D_{saw}w_{xx} + K_B v. \tag{4.8c}$$

Scaling these equations the same way as we did for the system (2.1) we have for U, V, W

$$\epsilon_1 \frac{\partial U}{\partial \tau} = \frac{\partial^2 U}{\partial y^2} - \mu_1 (U - V), \tag{4.9a}$$

$$\epsilon_2 \frac{\partial V}{\partial \tau} = \frac{\partial^2 V}{\partial y^2} + \mu_2 (U - V) - \beta_2 V, \tag{4.9b}$$

$$\epsilon_3 \frac{\partial W}{\partial \tau} = \frac{\partial^2 W}{\partial y^2} + \beta_3 V + F(\phi), \tag{4.9c}$$

where

$$F(\phi) = -\frac{\phi_a}{\gamma_m \phi_g(\phi_a\phi - \phi_b)}\frac{\partial \phi}{\partial \tau},$$

$$\frac{\partial \phi}{\partial \tau} = \frac{1}{\phi_a} W(y,\tau), \tag{4.10}$$

for $R = \phi_a\phi - \phi_b$. Also the nondimensional constants now are $\epsilon_1 = \frac{l^2}{D_{ha}t_0}$, $\mu_1 = K_T A_s \frac{\lambda_2 l^2}{\lambda_1 D_{ha}}$, $\epsilon_2 = \frac{l^2}{D_{hw}t_0}$, $\mu_2 = K_T A_s \frac{l^2}{D_{hw}}$, $\beta_2 = K_B \frac{l^2}{D_{ha}}$, $\epsilon_3 = \frac{l^2}{D_{saw}t_0}$, $\beta_3 = \frac{k_B \lambda_2 l^2}{D_{saw}\lambda_3}$ for $t_0 = \frac{C_c d}{K_c \lambda_3}$. In addition the boundary conditions have the following form

$$\phi(0,\tau)U(0,\tau) = 1, \qquad \left(\phi(1,\tau)U(1,\tau)\right)_y = 0, \tag{4.11a}$$

$$\phi(0,\tau)V(0,\tau) = 1, \qquad \left(\phi(1,\tau)V(1,\tau)\right)_y = 0, \tag{4.11b}$$

$$\phi(0,\tau)W(0,\tau) = 1, \qquad \left(\phi(1,\tau)W(1,\tau)\right)_y = 0, \tag{4.11c}$$

Finally at time $\tau = 0$ we have

$$U(y,0) = 0, \quad V(y,0) = 0, \quad W(y,0) = 0, \tag{4.12a}$$

$$\phi(y,0) = \phi_c. \tag{4.12b}$$

In Figure (9), the system of equations (4.9), (4.11) and (4.12) are solved numerically by applying the method given by equations (4.6) and (4.7). The upper free boundaries determined by the relation $R(y,\tau) = 1$ or $R(y,\tau) = \sqrt{2}$, indicating the points that R reaches one for the one - dimensional model and when R reaches $\sqrt{2}$ for the two - dimensional consideration and for configurations A and B, are plotted against time. In the case of the one - dimensional configuration the material takes more time to be fully transformed into gypsum compared with the case of configuration A and B with these being quite close during the process. Again we see no significant variation for the lower boundary which indicates when some point exceeds R_0. This means that the whole bulk of the material starts being corroded after the start of the phenomenon.

The Quasi Steady Approximation If we consider values of the parameters as in [4] we have again that $\mu_1, \mu_2 \gg 1$ and that $\epsilon_i \ll 1$, $i = 1,2,3$. Therefore a similar procedure can be applied as in Section 2 to obtain a simplified version of the model. To leading order terms we have $U \simeq V$ and the equations for V and W now have the form

$$\frac{\partial^2 V}{\partial y^2} - \beta_2 V = 0, \tag{4.13a}$$

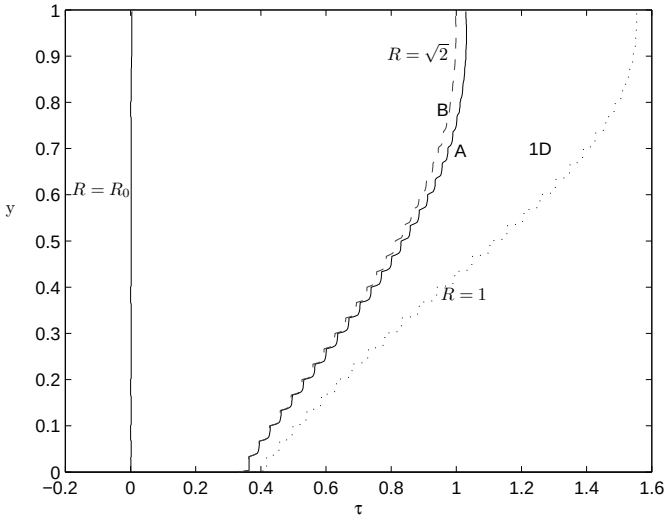

Fig. 9. *The free boundaries, given by the conditions* $R(\tau) = R_0$ *and* $R(\tau) = \sqrt{2}$*, are plotted against time after solving numerically the equations (4.9), (4.11) and (4.12), but with the source term given by equations (3.3) for the one - dimensional model, (3.6) for configuration A and (3.7) for configuration B, and with the boundary and initial conditions given by (4.11) and (4.12), for* $M = 31$*,* $\epsilon_1 = \epsilon_2 = \epsilon_3 = 1$*,* $\gamma_m = 1$*,* $\beta_1 = \beta_2 = 1$*,* $\mu_1 = \mu_2 = 1$*,* $\phi_c = 0.4$*,* $\phi_g = 0.6$*,* $\delta\tau = .8 \cdot \delta y^2$*.*

$$\frac{\partial^2 W}{\partial y^2} + \beta_3 V + F(\phi) = 0, \tag{4.13b}$$

combined with equation (4.10), the boundary conditions (4.11b) and (4.11c) and the initial condition for ϕ, (4.12b).

Finally the system of equations (4.13) is solved following the same numerical approach and the result is compared with the numerical solution of (2.15). The result in Figure (10) shows that throughout the process the distinct boundary $S(\tau)$, result of the Stefan-type model, remains at a low level (at 0.1 when $\tau \sim 1$) while according the mushy region - models the whole amount of the material is corroded. In the case of configuration A the material takes more time to be fully corroded compared with the one - dimensional model and the configuration B model and quite shorter time compared with the Stefan type model. The end of the simulation is specified when $S(\tau)$ and R intersect the line $y = 1$ for some times $\tau \sim 10$ and $\tau \sim .72$ respectively, i.e. the times that the whole of the material is corroded. This experiment indicates that the two - dimensional model, when configuration A is assumed, is the more realistic one, predicting larger time of corrosion, compared with the rest of the mushy region models presented in this work for this large diffusion limit where the quasi steady approximation is applicable.

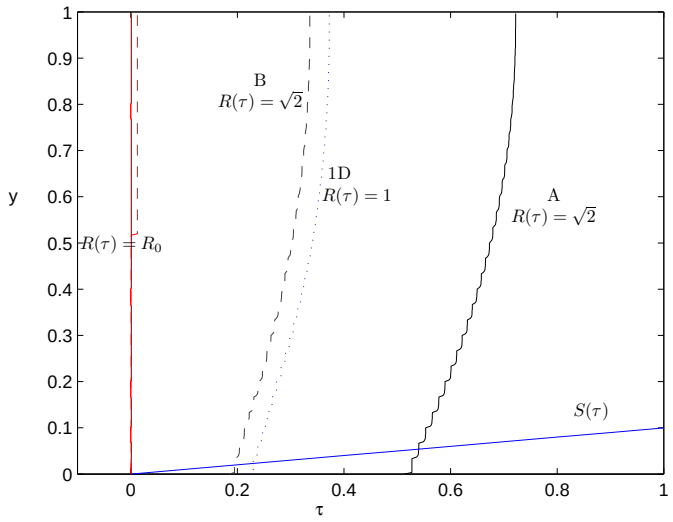

Fig. 10. *The free boundaries, given by the conditions* $R(y,\tau) = R_0$ *and* $R(y,\tau) = \sqrt{2}$*, and* $S(\tau)$ *are plotted against time after solving numerically the equations (4.9), (4.11) and (4.12), but with the source term given by equations (3.3) for the one - dimensional model, (3.6) for configuration A and (3.7) for configuration B, and with* $S(\tau)$ *given by (2.15). The boundary and initial conditions for the mushy region models are given by (4.11b, 4.11c), the last two of (4.12a) and (4.12b). The values of the parameters that were used were* $M = 31$*,* $\delta = 0.1$*,* $\gamma_m = 6.78$*,* $\gamma = 67.8$ $\beta_2 = 2.3275, \beta_3 = 2.3741\,10^{-5}$*,* $\phi_c = 0.2$*,* $\phi_g = 0.3$ $\delta\tau = 0.4 \cdot \delta y^2$*.*

5 Conclusions

In this work a mathematical model for the formation of a mushy region during corrosion by H_2SO_4 is constructed. The model is based in an already existing model for the corrosion of sewer pipes resulting in a Stefan problem. For this Stefan problem although an extensive analysis has been done in a series of papers by Böhm et all in [4] etc, an approximate solution is presented for a certain range of values of parameters corresponding to real situations as it is mentioned in [4]. The result is in very good agreement with these from [4].

As a next step a model is constructed allowing the formation of a mushy region, i.e. a region where the material is only partly corroded throughout the process. This more general model is derived via an averaging process of microscopic considerations, by the application of a method presented in [13] and has the form of a macroscopic phase field model. Variations of this model are presented in the case of a one - dimensional and two - dimensional considerations regarding the geometry of the cracks inside the concrete. The derived phase field models in their various forms, are solved numerically with a finite element scheme and the results, which predict corrosion within a reasonable range, are presented.

More complicated considerations of the geometry of cracks as well as their fractal structure, can be taken into account and lead to more realistic models. Furthermore other models accounting for the corrosion of the calcite near possible intersections of pores can be derived based on a combination of the one-dimensional model regarding corrosion away from the intersections and a two-dimensional model for the corrosion near the intersections. In addition variations of the scaling used in the multiple scales approach, for example when γ_m is not of order one, may result in interesting future extensions of this work.

References

[1] G. Ali, V. Furuholt, R. Natalini, I. Torcicollo, *A mathematical model of sulphite chemical aggression of limestones with high permeability. I. Modeling and qualitative analysis.* Transp. Porous Media **69**, no. 1, (2007), 109–122.

[2] G. Ali, V. Furuholt, R. Natalini, I. Torcicollo, *A mathematical model of sulphite chemical aggression of limestones with high permeability. II. Numerical approximation.* Transp. Porous Media **69**, no. 2, (2007), 175–188.

[3] N. De Belie, J. Montenya, A. Beeldensb, E. Vinckec, D. Van Gemertb,W. Verstraetec *Experimental research and prediction of the effect of chemical and biogenic sulfuric acid on different types of commercially produced concrete sewer pipes*, Cement and Concrete Research, **34**, no 12, (2004), 2223–2236.

[4] M. Böhm, J. Devinny, F. Jahani, G. Rosen, *On a moving-boundary system modelling corrosion in sewer pipes*, Applied Mathematics and Computation, **92**, (1998), 247–269.

[5] M. Bohm, J. S. Devinny, F. Jahani, F. B. Mansfeld, I. G. Rosen, C.Wang, *A Moving Boundary Diffusion Model for the Corrosion of Concrete Wastewater Systems: Simulation and Experimental Validation*, Proceedings of the Arnencan Control Conference San Diego, California, June 1999, 1739–1743.

[6] A. M. Brandt, G. Prokopski, *On the fractal dimension of fracture surfaces of concrete elements*, Journal of Materials Science, **28**, no 17, (1993), 4762–4766.

[7] B Chiaia, J. G. M. van Mier, A. Vervuurt, *On the fractal dimension of fracture surfaces of concrete elements*, Cement and Concrete Research, **28**, no 1, (1998), 103–114.

[8] A. Fasano, R. Natalini *Lost Beauties of the Acropolis : What Mathematics Can Say*, SIAM News, **39**, July/August 2006.

[9] C. Giavarini, M. L. Santarelli, R. Natalini, and F. Freddi, *A nonlinear model of sulfa- tion of porous stones: Numerical simulations and preliminary laboratory assessments* J. Cultural Heritage, **9**, (2008), 14–22.

[10] F.R. Guargualini, R. Natalini *Global Existence of solutions to a nonlinear model of sulphasion phenomena in calcium carbonate stones*, Nonlinear Analysis : Real World Applications, **6**, (2005), 477–494.

[11] G. M. Idorn *Innovation in concrete researchreview and perspective*,Cement and Concrete Research, **35**, (2005), 3–10.

[12] A. Muntean, M. Böhm, *A moving-boundary problem for concrete carbonation: global existence and uniqueness of weak solutions.* J. Math. Anal. Appl. **350**, no. 1, (2009), 234–251.

[13] A.A Lacey, L.A. Herraiz *Macroscopic models for melting derived from averaging microscopic Stefan problems I: Simple geometries with kinetic undercooling or surface tension* . Euro. Jnl. of Applied Mathematics, **11**, (2002), 153–169.

[14] A.A Lacey, L.A. Herraiz *Macroscopic models for melting derived from averaging microscopic Stefan problems II: Effect of Varying geometry and composition.* Euro. Jnl. of Applied Mathematics, **13**, (2002), 261–282.